Electronic Supplementary Material (ESI) for Nanoscale Horizons.

Supporting Information

3D computer-aided nanoprinting for solid-state nanopores

Haibo Ding[a,b], *Qiming Zhang*[a], *Zhongze Gu*[b], *Min Gu*[a]

[a]Laboratory of Artificial-Intelligence Nanophotonics, School of Science, RMIT University, Melbourne, VIC 3001, Australia;

[b]State Key Laboratory of Bioelectronics, School of Biological and Medical Engineering, Southeast University, Nanjing 210096, China.

E-mail address: min.gu@rmit.edu.au

Figures:

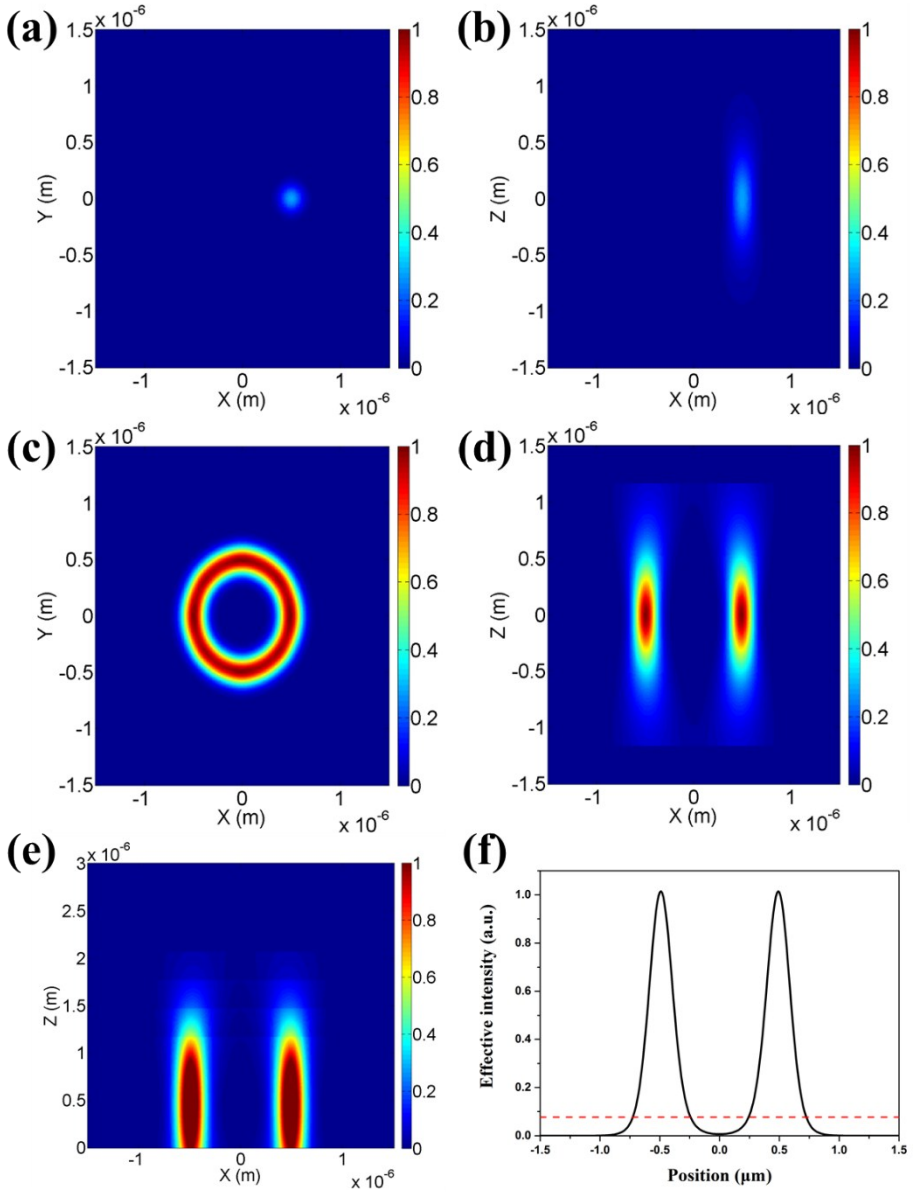

Figure S1. (a, b) Normalized distribution of exposure doses for single focal spot in the (a) XY plane (z= 0) and (b) XZ plane (y=0). (c, d) Normalized distribution of exposure doses of 50 focal spots in single circular path in the (c) XY plane (z= 0) and (d) XZ plane (y=0). (e) Normalized distribution of exposure doses for four scanning paths in the XZ plane. (f) Normalized distribution of exposure doses for four scanning paths along the X axis when z= 0 and y=0.

.

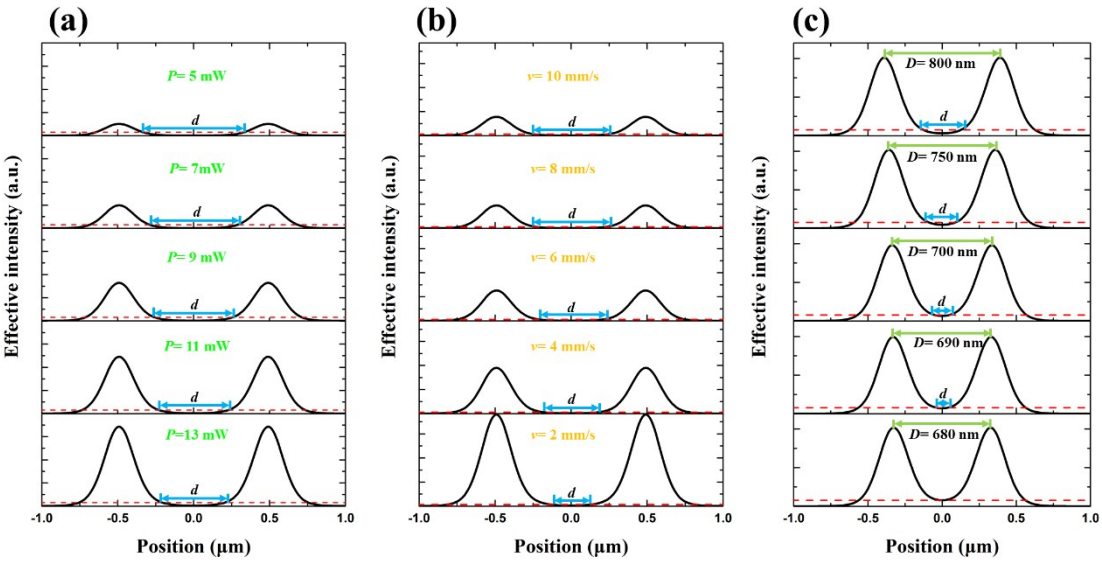

Figure S2. (a) Schematic demonstration of reducing the diameter of nanopores by increasing the laser power. (b) Schematic demonstration of reducing the diameter of nanopores by reducing the scanning speed. (c) Schematic demonstration of reducing the diameter of nanopores by reducing the diameter of the scanning path. Normalized distribution of exposure doses along the X axis when z= 0 and y=0.

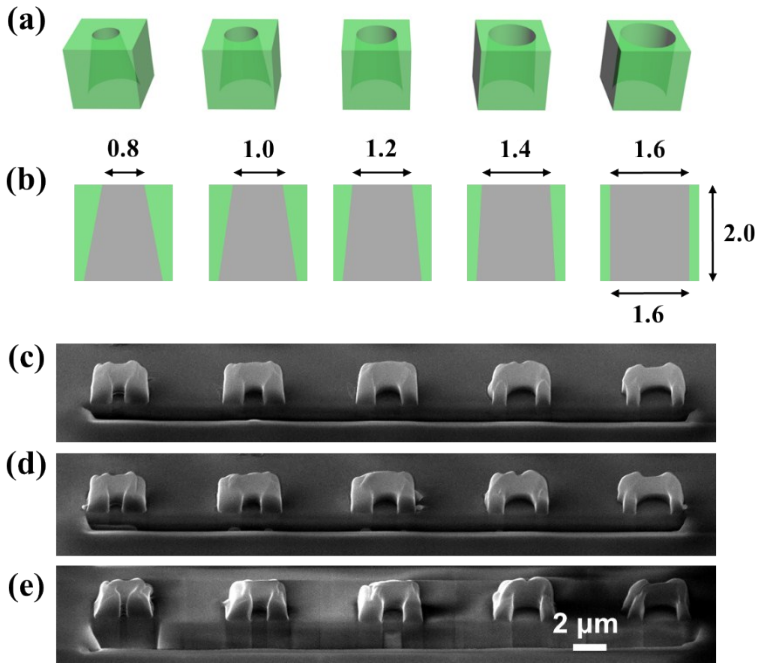

Figure S3. (a) 3D models of the nanopores with different asymmetric shapes. (b) Geometric parameters of these asymmetric shapes with a unit of μm. SEM images of the fabricated nanopores with different shapes and varying slicing distance in Z direction of 300 nm (c), 200 nm (d) and 100 nm (e).

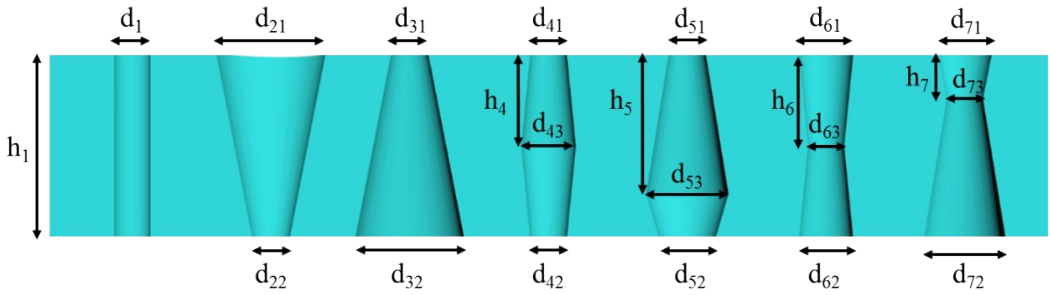

Figure S4. Geometric design of the seven nanopores.

Table S1 Geometric parameters of the seven nanopores.

Parameter	Unit	Value
d_1	nm	800
d_{21}	nm	2400
d_{22}	nm	800
d_{31}	nm	800
d_{32}	nm	2400
d_{41}	nm	800
d_{42}	nm	800
d_{43}	nm	1200
d_{51}	nm	800
d_{52}	nm	1200
d_{53}	nm	1800
d_{61}	nm	1200
d_{62}	nm	1200
d_{63}	nm	800
d_{71}	nm	1200
d_{72}	nm	1800
d_{73}	nm	800
h_4/h_1		0.5
h_5/h_1		0.75
h_6/h_1		0.5
h_7/h_1		0.25
h_1	nm	1000, 2000, 6000

Discussion:

Numerical models of the diameter of nanopores:

The entire exposure doses are calculated by the sum of the intensity's squares of all the focal spots along the fabrication path. The intensity distribution of each focal spot could be described as[1]:

$$I(x,y,z) = \frac{I_0}{1 + z^2/z_0^2} e^{\frac{-2(x^2+y^2)}{\omega_0^2(1+z^2/z_0^2)}} \quad \text{(S-1)}$$

where I_0 is the peak irradiance at the focal spot, ω_0 is the beam waist at the focal spot, and z_0 is the corresponding Rayleigh length. Here, the peak irradiance at the focal spot could be calculated by the power (P), the pulse width (τ), the repetition rate (f) of the laser:

$$I_0 = \frac{2P}{\pi\omega_0^2\tau f\sqrt{\pi}} \quad \text{(S-2)}$$

The unit of I_0 is GW/cm^2. Besides, the beam waist and the corresponding Rayleigh length of the focal spot with a 3D Gaussian distribution could be calculated as 480 nm and 1040 nm[2]. Considering the accumulation effect, the boundary conditions for each focal spot are set at $[-\sqrt{5}\omega_0, \sqrt{5}\omega_0]$ in the XY plane and $[-\sqrt{5}z_0, \sqrt{5}z_0]$ in the Z direction.

Figure S1a, b show the calculated results for the focal spot which is located at the position (500 nm, 0, 0).

The number of focal spots along a circular scanning path (n) could be calculated as:

$$n = \frac{C}{v\tau} \tag{S-3}$$

where C is the circumference of the circular path, v is the scanning speed. To simplify the calculation, we assumed the number is 50 when the diameter of scanning path is 1000 nm and the scanning speed is 10 mm/s.

Figure S1c and d show the calculated results for 50 focal spots which are located along the circular path with a diameter of 1000 nm at focus plane.

Figure S1e show the calculated results for 4 scanning paths with a slicing distance of 300 nm. There are 200 focal spots in total.

To predict the diameter of the generated nanopores, we extracted the distribution of exposure dose along the X axis when z= 0 and y=0 (Figure 1f). The simulation results were normalized by dividing the index of 3000000 and the diameter was obtained by a threshold value of 0.077.

To simulate the effect of the laser power (P), the diameter of the scanning path was 500 nm and the scanning speed was 10 mm/s. Some typical images were shown in Figure S2a. The simulation data and the experimental results can be fitted with an empirical formulas:

$$d = d_0 + k \times e^{-\frac{P - P_0}{q}} \tag{S-4}$$

where $d_0 = 207$ nm, $k = 471$ nm/mW, $P_0 = 4.77$ mW, $q = 9.79$.

To simulate the effect of the scanning speed (v), the laser power was 10 mW and the diameter of the scanning path was 500 nm. Some typical images were shown in Figure S2b. The simulation data and the experimental results can be fitted with an

empirical formulas:

$$d = d_0 + k \times e^{-\frac{v - v_0}{q}} \quad \text{(S-5)}$$

where $d_0 = 490$ nm, $k = -3.87 \times 10^{-4}$ s, $v_0 = 0.900$ mm/s, $q = 2.85$.

To simulate the effect of the diameter of scanning path (D), the laser power was 10 mW and the scanning speed was 10 mm/s. Some typical images were shown in Figure S2c. The simulation data and the experimental results can be fitted with three empirical formulas:

$$d = \alpha \times (D - D_{lim})^{\beta} \quad \text{(S-6)}$$

where $\alpha = 17.3$, $\beta = 0.561$, $D_{lim} = 680$ nm. Here, D_{lim} is the lower limit of the diameter of the scanning path for the fixed laser power and scanning speed. α and β are parameters related to the fabrication conditions and the photoresists.

Effect of the slicing distance:

The slicing distance also has an effect on the final shape of the nanopores due to the memory effect along the Z axis. We fabricated five nanopores embedded in a cubic structure for the comparison of different slicing distance for complex shapes (Figure S3). For the objects with the same height, the slicing distance of 100 nm brings more extra polymerization in the central zone, leading to a distortion of the desired shape. Moreover, a smaller slicing distance requires a longer fabrication time for the same object. Consequently, the slicing distance is fixed as 300 nm throughout this paper.

Reference:

1. Cheng, Y.; Sugioka, K.; Midorikawa, K.; Masuda, M.; Toyoda, K.; Kawachi, M.;

Shihoyama, K. *Opt. Lett.* **2003**, *28* (1), 55-57.

2. Urey, H. *Appl. Opt.* **2004**, *43* (3), 620–625.